Spectroscopic, biological activity and scanning electron microscope studies of Pd (ii) with Tetrazole-thione and Phosphines complexes

Abdullah A. Yaseen*, and *Amenah* I. A. Al-Nassiry

Department of Chemistry, College of Education for Pure Science, University of Tikrit, Tikrit, 34001 Iraq

Abstract. Five mixed-ligand phenyl Palladium (II) complexes containing 5-benzylthion-1H-tetrazole (LH) and phosphines (1-5) were synthesized. These complexes are classified into one groups: [PdL2(dppm)], [PdL2(dppe)], [PdL2(dppp)], [PdL2(dppb)], [PdL2(dppf)], (1,5). The complexes were prepared with moderate to high yields and characterized by various techniques. The characterization data indicated that the L-ligand acts a monodentate ligand through the nitrogen atom in the tetrazole ring in complexes (1-5), adopting a square planar geometry around the Pd(II) center. The crystal structure of the complexes was examined using scanning electron microscopy (SEM), and the results revealed the presence of normal nanostructures.

1 Introduction

Tetrazole is a cyclic organic compound (a heterocyclic ring) consisting of a five-membered ring made up of four nitrogen atoms, one carbon atom, and two hydrogen atoms. Its molecular formula is CH_2N_4. It appears as a light yellow crystalline solid with a distinctive aromatic odor. Tetrazole is soluble in alcohol and water and exhibits acidic properties due to the presence of a hydrogen atom attached to one of the nitrogen atoms [1]. They are extensively utilized in the pharmaceutical industry because of their notable biological activity [2]. Tetrazoles exist in two tautomeric forms:

The most common method for preparing the tetrazole ring is by adding hydrazoic acid or azide to compounds containing an unsaturated nitrogen bond, such as Thiocyanate, Cyanates, Imines-Carbodi, and Cyanides. During this reaction, the intermediate compound

* Corresponding author : aayueps114@st.tu.edu.iqs

is formed from imideazides, which undergoes a ring closure to form the tetrazole ring.[3], as below:

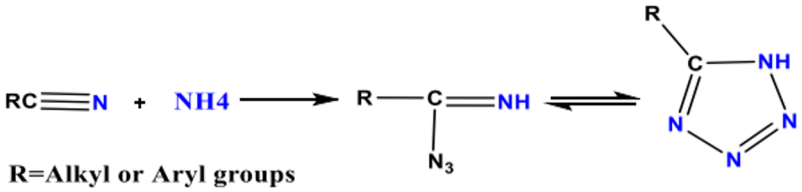

Tetrazole-thione complexes are coordination compounds formed by the binding of tetrazole-thione ligands to a central metal atom. These ligands are derived from tetrazole compounds in which one of the nitrogen atoms is replaced by a sulfur atom (S). These complexes have attracted significant interest due to their diverse coordination behavior and potential applications across various fields [4-8] . Tetrazole-thione ligands are characterized by the presence of a tetrazole ring (-C-N-N-N) and a thione moiety (C-S). Thetetrazole ring can have substituents at different positions, influencing the coordination properties and reactivity of the ligand. Tetrazole thione ligands can coordinate with a variety of metal ions, including transition metal ions such as Cu(II), Pd(II), Pt(II), Hg(II), Zn(II), Co(II), Fe(II), etc., this coordination happens via the nitrogen atoms of the tetrazole ring and the sulfur atom of the thione group [9-13] . Compounds containing the tetrazole ring have occupied a wide space in the field of pharmaceutical compounds, as this ring is included in the synthesis of a number of antibiotics such as cefazolin[14] and ceftizol[15]. Tetrazole compounds have a wide spectrum of biological activity, as they are effective against diabetes and effective against bacteria.

2 Experimental section

2.1. Materials and methods

All the chemicals, reagents and solvents for the synthesis of compounds were supplied and used without more purification. The melting point of the prepared complexes was recorded on Automatic (SMP30) melting point apparatus. The molar conductivity of 10^{-3} M freshly DMSO solution of prepared complexes was measured using (Starter 3100c) digital conductivity meter at 25°C. The IR spectra of the prepared complexes as KBr pellets were recorded using a Shimadzu FT-IR 8400S spectrophotometer (400-4000 cm^{-1}). NMR spectra were acquired on a Bruker 400 MHz spectrometer in DMSO-d6 as a solvent. The isolates of the pathological bacteria that were used in the research obtained from the laboratories of the Department of Life Sciences in the College of Education for Pure Sciences at the University of Tikrit.

2.1.1 Preperation of [PdL_2]

A colorless solution of KOH (0.0381 g, 0.679 mmol) dissolved in 5 mL of absolute ethanol was added to a colorless solution of (LH) (0.13 g, 0.679 mmol) dissolved in 5 mL of absolute ethanol. This mixture was then added to a brown solution of Na2PdCl4 (0.1 g, 0.339 mmol) dissolved in 5 mL of absolute ethanol, resulting in the formation of a yellow precipitate. The mixture was stirred continuously for two and a half hours and and dried under vacuum to give a Yellow powder. {Yield = 0.143 g, 89%, m.p (°C) = 193-195}.

2.1.2 Preperation of [PdL2(dppm)]

A hot solution of KOH (0.0381g , 0.671mmol) in EtOH (5 ml) was added to hot solution of 5-benzylthion-1H-tetrazole (LH) ligand (0.13 g; 0.679 mmol) in EtOH (5 ml) was added to a solution of Sodium Tetrachloropalladate (II) (0.100 g , 0.339 mmol) in EtOH (5 ml), with stirred for 2 h ,then a yellow ppt. was formed direct. The mixture was stirred for 3 h, then filtered off, washed with distal water for several times, and dried under vacuum to give a yellow powder {Yield = 0.2147 g, 72%, m.p (ºC) = 179-181}. The [PdL_2(dppe)] (2), [PdL_2(dppp)] (3), [PdL_2(dppb)] (4), [PdL_2(dppf)] (5) was prepared and isolated by similar method. See Table 1 and Figure 1.

Table 1. Results of electrical conductivity and molarity measurements, some physical properties, and yield percentages of the prepared ligand and metal complexes.

Seq	**Complexes**	**Color**	**m.p(ºC)**	**Yield %**		**Conductivity ohm^{-1}.cm^{-2} .mol^{-1}**
1	LH	White	135-138	-	-	4.1
2	[PdL_2]	Yellow	193-195	0.143g	%89	4.2
3	[PdL_2(dppm)]	Dark yellow	179-181	0.2147g	%72	4.58
4	[PdL_2(dppe)]	Light yellow	151-153	0.2231g	%74	4.33
5	[PdL_2(dppp)]	Light yellow	157-159	0.2348g	%76	5.97
6	[PdL_2(dppb)]	Light yellow	157-159	0.2439g	%78	9.18
7	[PdL_2(dppf)]	Orange	167-169	0.2982g	%84	7.68

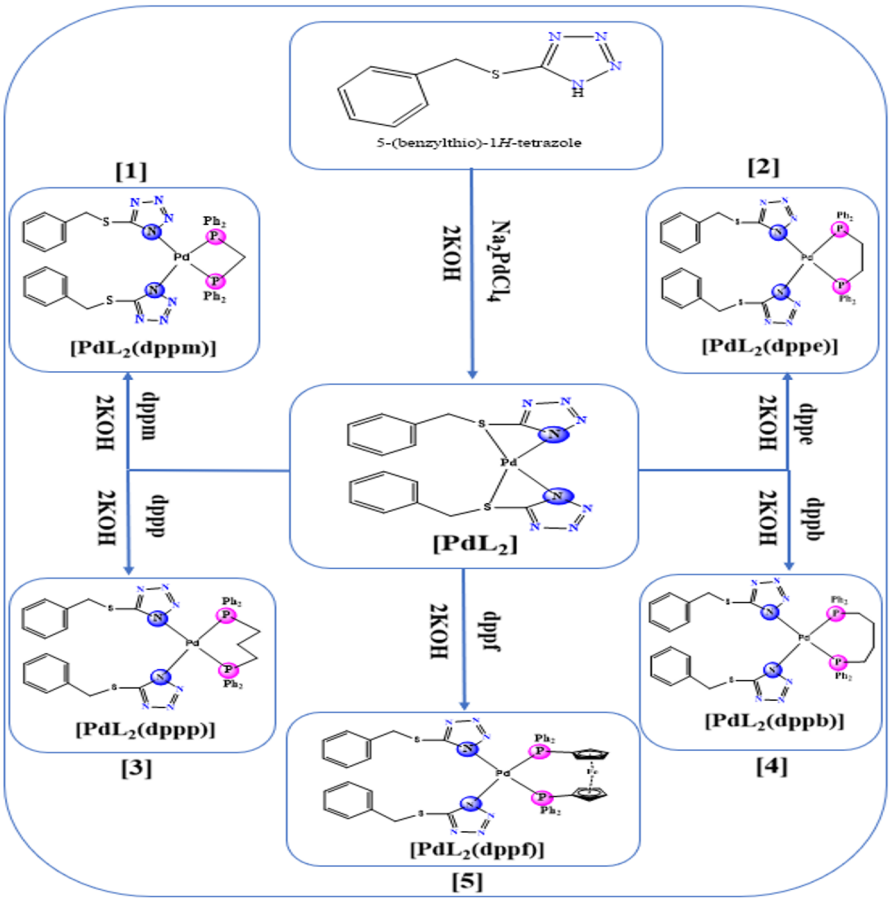

Fig. 1. Pd (II) Complexes with Ligand (L) and Phosphines.

3 Results and discussion

3.1 Synthesis and characterization

Treatment of two molar of 5-benzylthion-1H-tetrazole ligand (L) and Na_2PdCl_4 afforded a white ppt characterized as a [PdL_2] in high yield (89%) . The [PdL_2] complex was treated with equivalent mole of diphosphine {$Ph_2P(CH_2)nPPh_2$} {where n = 1 dppm, 2 dppe, 3 dppp, 4 dppb, $(CH_2)n = (Cp)_2Fe$}. The resulting compounds were characterized by IR, ^{1}H-NMR, ^{31}P-{1H} NMR, molar conductivity measurements, and elemental analysis. The conductivity measurements data displayed that complexes have a low conductivity value and fell within the range of non-electrolyte. The ^{31}P-{^{1} H} NMR spectra of complexes (1-5) (Figure 2) displayed a single signal, confirming equivalent phosphorus atoms and the formation of a single isomer for each complex.

[PdL_2]: Yellow powder, (0.143 g), yields 89%, m.p : 193-195ºC. FTIR(KBr): 3061m ν(C-H)Ar., 2928m ν(C-H)alip., 1629s ν(C=N), 1492 υ(C=C), 1381m ν(N=N), 1242s ν(N-N), 769m ν(C-S). ^{1}H NMR: (DMSO-d6) δ(ppm): 7,47 (d, 3JH-H = 8.23 Hz, 4H, Ha), 7.32 (t, (4JH-H= 7.76 Hz,3JH-H= 1.26 Hz) 4H, Hb), 7.12 (t, 4JH-H= 7.09 Hz,3JH-H= 1.25

Hz,2H, Hc), 3.97(s, 4H,CH_2). ^{13}C-{^1H}-NMR**:** 144.20 (C_1), 128.68 (C_2), 125.48 (s,C_3), 121.80 (s,C_4), 111.39 (m,C_5), 32.30 (m,C_6).

[PdL$_2$(dppm)]: Dark Yellow powder, (0.2147g), yields 72%, m.p : 179-181^{o}C,FTIR(KBr): 3059m ν(C-H)Ar., 2978m ν(C-H)aliph, 1620s ν(C=N), 1492s υ(C=C), 1435s ν(P-Ph), 1379s ν(N-N), 738m ν(C-S), 700s ν(P-C).^{1}H NMR (DMSO-d6) δ(ppm): 7,38 (d, 3JH-H = 7.75 Hz, 4H, Ha), 7.24 (b, 12H, HPh), 7.30 (t, 4JH-H= 7.16 Hz,3JH-H= 1.27 Hz ,4H, Hb), 7.09 (t, 4JH-H= 7.55 Hz,3JH-H= 1.25 Hz ,2H, Hc), 7.16 (b, 8H, HPh), 4.00 (s, 4H, CH_2L), 3.03 (4JP-H= 1.76 Hz, t, 2H, CH_2dppm). ^{31}P{^1H}NMR δPA= -52.31 ppm .

[PdL$_2$(dppe)]: Light Yellow powder, (0.2231g), yields 74%, m.p : 179-181^{o}C,FTIR(KBr): 3057m ν(C-H)Ar., 2960m ν(C-H)aliph, 1620s ν(C=N), 1481s υ(C=C), 1435s ν(P-Ph), 1359s ν(N-N), 771m ν(C-S), 698s ν(P-C). ^{1}H NMR (DMSO-d6) δ(ppm): 7,39 (d, 3JH-H = 8.12 Hz, 4H, Ha), 7.32 (m, 12H, HPh), 7.30 (t, 4JH-H= 7.49 Hz,3JH-H= 1.21 Hz ,4H, Hb), 7.14 (t, 2H, Hc), 7.09 (b, 8H, HPh), 3.98 (s, 4H,CH_2), 3.11 (t, 4H, CH_2dppe).^{31}P{1H}NMR δP= 66.68 ppm (s).

[PdL$_2$(dppp)]: Light Yellow powder, (0.2348g), yields 76%, m.p : 135-138^{o}C,FTIR(KBr): 3055m ν(C-H)Ar., 2935m ν(C-H)aliph, 1616s ν(C=N), 1499s υ(C=C), 1435s ν(P-Ph), 1356s ν(N-N), 748m ν(C-S), 696s ν(P-C). ^{1}H NMR (DMSO-d6) δ(ppm): 7,38 (d, 3JH-H = 7.81Hz, 4H, Ha), 7.30 (t, 4JH-H= 7.28 Hz,3JH-H= 1.28 Hz ,4H, Hb), 7.14 (t, 4JH-H= 7.51, 3JH-H= 1.22 Hz ,2H, Hc), 7.12 (b, 20H, HPh), 4.00 (s, 4H,CH_2), 3.01 (t, 2H, CH_2dppp), 2.83 (t, 4H, CH2dppp).^{31}P{1H}NMR δP= 29.99 ppm(s).

[PdL$_2$(dppb)]: Light Yellow powder, (0.2439g), yields 78%, m.p : 179-181^{o}C,FTIR(KBr): 3057m ν(C-H)Ar., 2928m ν(C-H)aliph, 1622s ν(C=N), 1492s υ(C=C), 1433s ν(P-Ph), 1377s ν(N-N), 730m ν(C-S), 698s ν(P-C). ^{1}H NMR (DMSO-d6) δ(ppm): 7,42 (d, 3JH-H = 8.08 Hz, 4H, Ha), 7.30 (b, 12H, HPh), 7.28 (t, 4JH-H= 7.42 Hz,3JH-H= 1.16Hz ,4H, Hb), 7.20 (t, 4JH-H= 7.48,3JH-H= 1.18Hz, 2H, Hc), 7.15 (m, 8H, HPh), 3.99 (s, 4H,CH_2L), 3.04 (t, 4H, CH_2dppb), 2.82 (t, 4H, CH_2dppb).^{31}P{1H}NMR δP= 38.66 ppm (s).

[PdL$_2$(dppf)]: Orange powder, (0.2982g), yields 84%, m.p : 167-169^{o}C,FTIR(KBr): 3055m ν(C-H)Ar., 2960m ν(C-H)aliph, 1629s ν(C=N), 1479s υ(C=C), 1431s ν(P-Ph), 1379s ν(N-N), 769m ν(C-S), 744s ν(P-C). ^{1}H NMR (DMSO-d6) δ(ppm): 7,37 (d, 3JH-H = 7.98 Hz, 4H, Ha), 7.22 (m, 12H, HPh), 7.20 (t, 4JH-H= 7.40 Hz,3JH-H= 1.16 Hz ,4H, Hb), 7.10 (t, 4JH-H= 7.48 Hz,3JH-H= 1.20Hz ,2H, Hc), 7.08 (m, 8H, HPh), 4.02 (s, 4H,CH_2L), 3.81(m, 4H, CHcp), 3.69 (m, 4H, CHcp).31P{1H}NMR δP= 29.33 ppm (s).

IR data

The infrared spectrum of the complex [Pd(LH)$_2$] showed the disappearance of the N-H band that was present in the used ligand shown in Figure (3). The spectrum of the complex showed the presence of a band at the frequency (1629 cm^{-1}) dating back to the stretch of ν(C=N), the appearance of a band at (1492cm^{-1}) is attributed to the stretching of the group ν(C=C)[20], and the band at frequency (1381cm^{-1}) is due to the stretching of the group ν(N=N) [14], and the appearance of a band Also at (1242cm^{-1}) it was attributed to the ν(N-N) stretch[21], and it also showed a band at the frequency (769cm^{-1}) that was attributed to the ν(C-S) stretch, in addition to the frequency (3059cm^{-1}) which belongs to the ν(C-H) aromatic and the frequency (2929cm^{-1}) belongs to the aliphatic ν(C-H) stretch and the appearance of a band at frequency (476cm^{-1}) belongs to the ν(Pd-N) group.

While the infrared spectrum of the prepared complexes showed a new signal between the range (1431 s - 1435 s) and (698s – 700s) attributed to υ(P-Ph) and υ(P-C), respectively, and a signal within the range (1616 s -1629 s), attributed to υ(C=N) group, and a signal within the range (2929 m - 2978 w), (3028 s - 3055 m) attributed to Alph.υ(C-H) and Ar υ(C-H) [15].

SEM and EDX

The recent studies on the geometry of coordinate compounds have shown that most of them can be systematically produced nano-sized engineering structures [14]. In this paper, the morphological appearance of the microstructure of some complexes prepared by SEM technology was studied.

The SEM analysis of the complex [PdL_2(dppe)], shown in Figure (2-a), revealed the presence of nanostructured aggregates with irregular shapes. The images were captured using a cross-sectional area of 500 nm and a magnification power of 5.0Kx.

The particle sizes were analyzed using a Gaussian Fit curve, as illustrated in Figure (2-b). The results indicated that the average particle diameter was 95.42 nm, confirming its classification as a nanostructure. The standard deviation of the particle diameters was 1.41 nm, reflecting a relatively narrow size distribution.

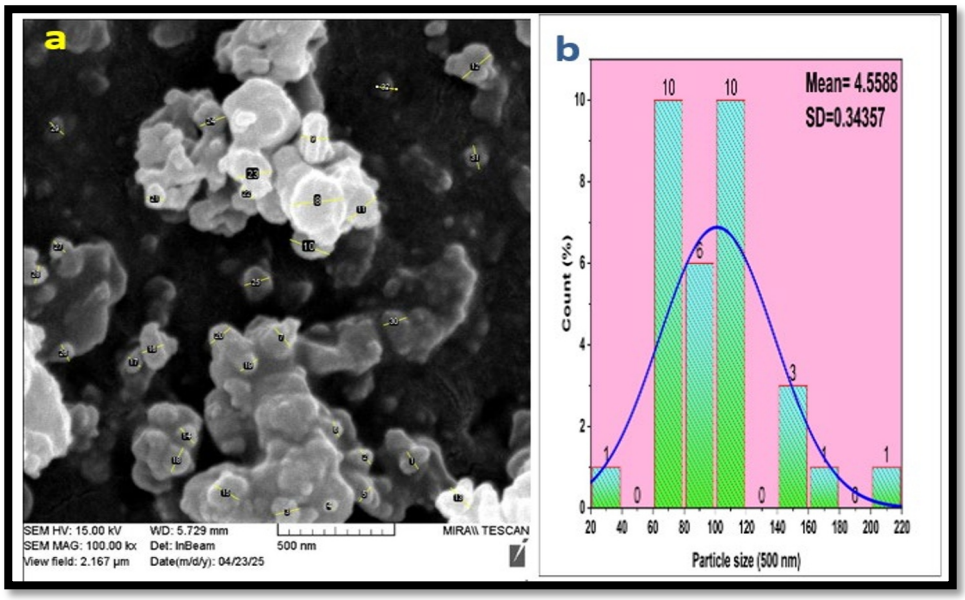

Fig. 2. (a) SEM image of the complex [PdL_2(dppe)] at 500 nm., (b) Particle size distribution and Gaussian Fit curve for the complex [PdL_2(dppe)] at 500 nm.

The EDX analysis of the complex [PdL_2(dppe)] for the SEM image at a size of (10 µm) and magnification (MAG: 3.00Kx), as shown in Figure (3), indicates that the peaks correspond to the elements C, Pd, N, S, and P, which are the constituent elements of the prepared complex.

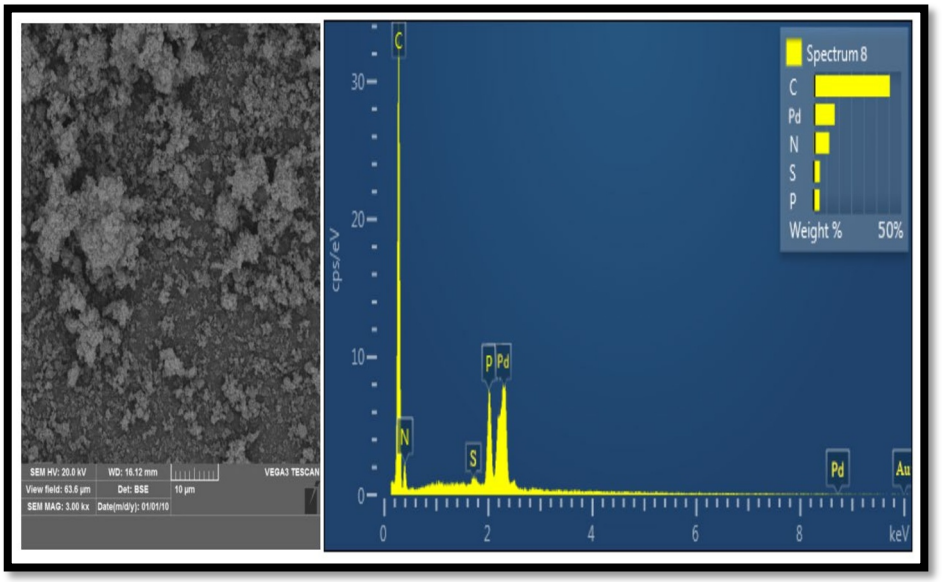

Fig. 3. The Energy dispersive X-Ray spectroscopy (EDX) analysis of the complex [PdL_2(dppe)].

The SEM analysis of the complex [PdL_2(dppp)], shown in Figure (4-a), revealed the presence of irregular and fused nanostructured aggregates. The analysis was conducted using a cross-sectional area of 500 nm and a magnification power of 70.0Kx.
Particle sizes were analyzed using a Gaussian Fit curve, as illustrated in Figure (4-b). The results showed that the average particle diameter was 82.63 nm, confirming its classification as a nanostructured aggregate. The standard deviation of the particle diameters was 1.50 nm, indicating a relatively narrow size distribution.

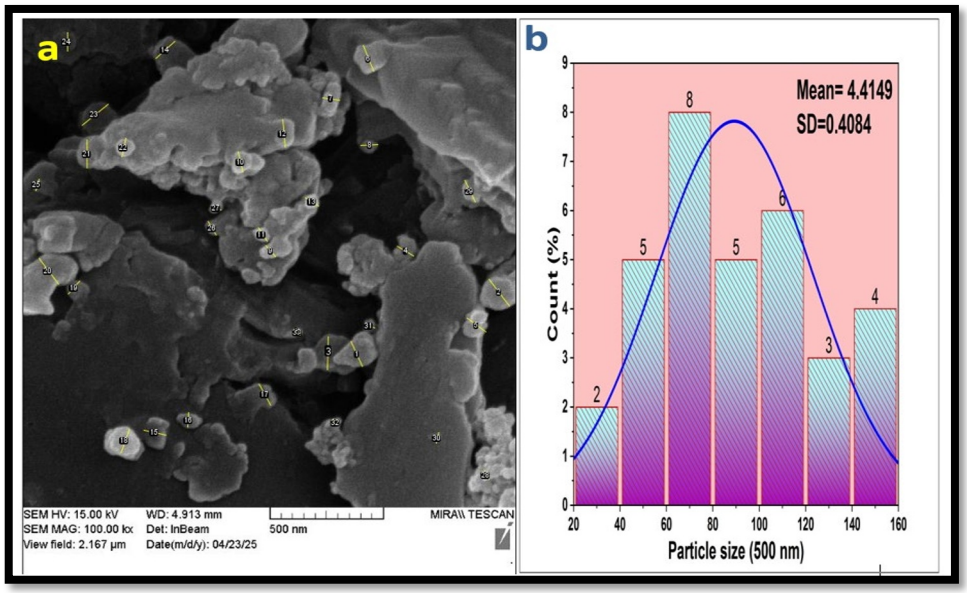

Fig. 4. (4-a) SEM image of the complex [PdL_2(dppp)] at 500 nm, and (b) Particle size distribution and Gaussian Fit curve for the complex [PdL_2(dppp)] at 500 nm.

The SEM analysis of the complex [PdL_2(dppf)], shown in Figure (5-a), revealed the presence of nanostructured aggregates with irregular shapes. The analysis was conducted using a cross-sectional area of 500 nm and a magnification power of 5.0Kx.
The particle sizes were analyzed using a Gaussian Fit curve, as illustrated in Figure (5-b). The results indicated that the peak particle diameter was 84.40 nm, placing it within the nanoscale range. The standard deviation of the particle diameters was 1.34 nm, indicating a relatively narrow size distribution.

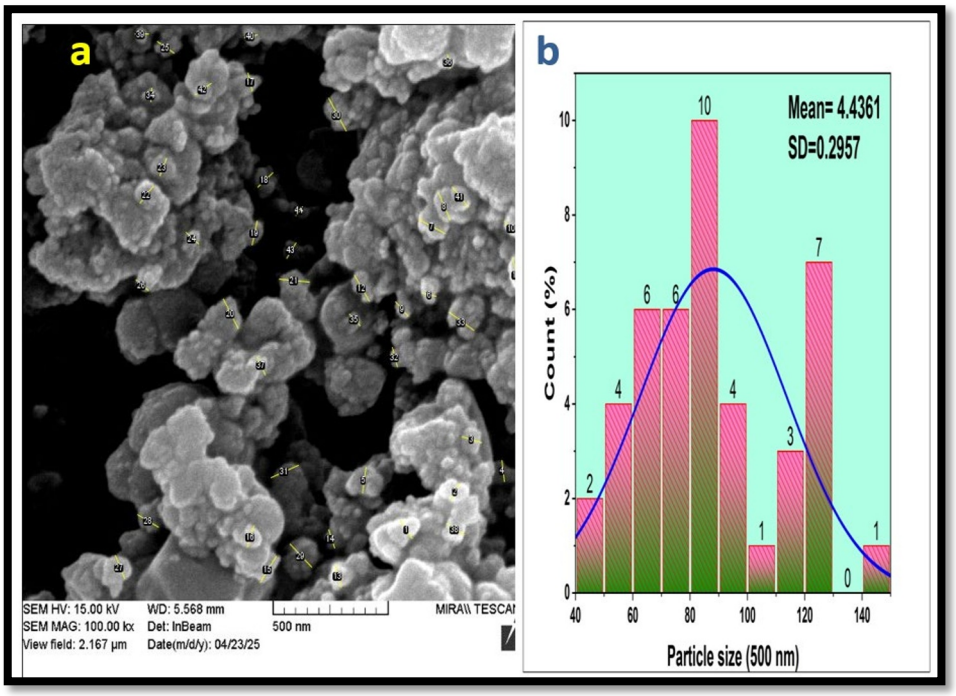

Fig. 5. (a) SEM image of the complex [PdL_2(dppf)] at 500 nm, and (b) Particle size distribution and Gaussian Fit curve for the complex [PdL_2(dppf)] at 500 nm.

The EDX analysis of the complex [PdL_2(dppf)] for the SEM image at a size of (10 µm) and magnification (MAG: 3.00 Kx), as shown in Figure (5-c), revealed that the peaks correspond to the atoms C, Pd, Fe, P, N, and S, which are the constituent elements of the complex.

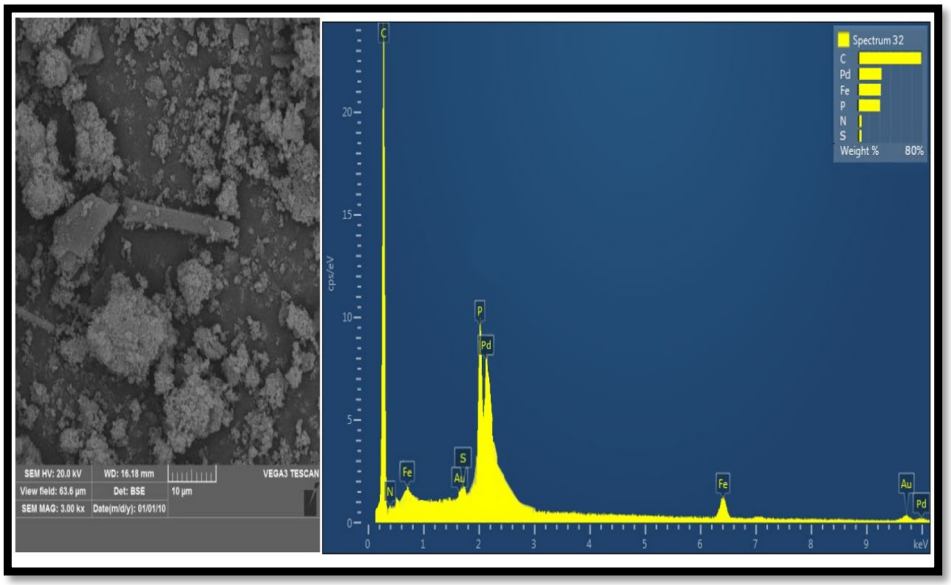

Fig. 5. (c) The Energy dispersive X-Ray spectroscopy (EDX) analysis of the complex [PdL2(dppf)].

These results are good results in the field of coordination chemistry, as they open up prospects for the usability of complexes in a wide range of applications. Regarding the results obtained, the measurements proved the existence of regular nanostructures with high porosity, which means that these compounds are able to be used in applications requiring a high porosity surface area, such as those required in hydrogen storage applications. Although the compositions of nanocomplexes were addressed infrequently the SEM results in this study are consistent with the previously published results indication the possibility to synthesize complexes containing nanostructures. It was also revealed that the particle sizes in this study were somewhat larger than those previously reported.

3.2 Biological activity evalution

The bacterial activity of the prepared complexes was tested on two types of gram-negative bacteria Escherichia coli and Acinetobacter baumannii and gram-positive bacteria Staphylococcus aureus (s.a) and Streptococcus faecali(S.f), where the results showed that the Palladium complexes gave a good and varying inhibition rate according to the concentrations used. See Table 2 and Figure 6. The mechanism may involve an affinity between the complex and the bacterial surface, resulting in an association between the heterogeneous atoms of the cell membrane with palladium, causing a change in the cell wall that inhibits bacterial growth and separation.

Table 2. The inhibitory activity of some prepared compounds against four types of Gram-positive and Gram-negative bacteria (Inhibition Zone (mm)).

N	Complexes	Cone	Staphylococcus aureus (+)	Streptococcus faecali(+)	*Escherichia coli(-)*	Acinetobacter baumanii(-)
1	[PdL_2]	10^{-3}	11	15	6	12
		10^{-4}	9	5	NIZ	8
		10^{-5}	3	2	NIZ	10
2	[PdL_2(dppm)]	10^{-3}	6	12	11	10
		10^{-4}	NIZ	NIZ	2	4
		10^{-5}	NIZ	NIZ	NIZ	NIZ
3	[PdL_2(dppe)]	10^{-3}	8	7	7	6
		10^{-4}	7	NIZ	3	4
		10^{-5}	NIZ	NIZ	NIZ	3
4	[PdL_2(dppp)]	10^{-3}	4	10	12	4
		10^{-4}	2	4	3	NIZ
		10^{-5}	2	NIZ	NIZ	2
5	[PdL_2(dppb)]	10^{-3}	14	8	5	10
		10^{-4}	11	9	NIZ	4
		10^{-5}	2	4	NIZ	3
6	[PdL_2(dppf)]	10^{-3}	9	12	6	14
		10^{-4}	6	4	NIZ	7
		10^{-5}	NIZ	NIZ	NIZ	4

* NIZ (Non Inhibition Zone)

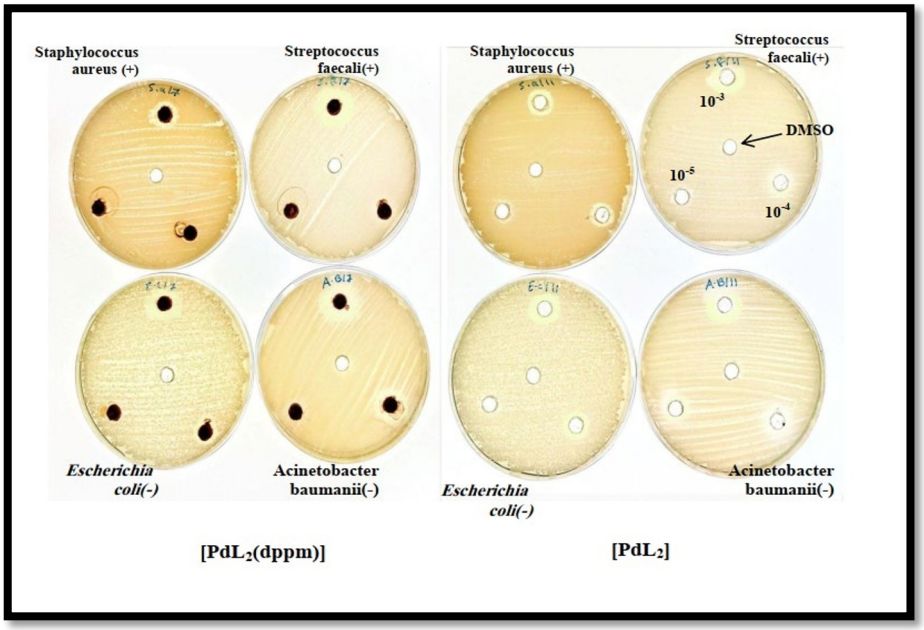

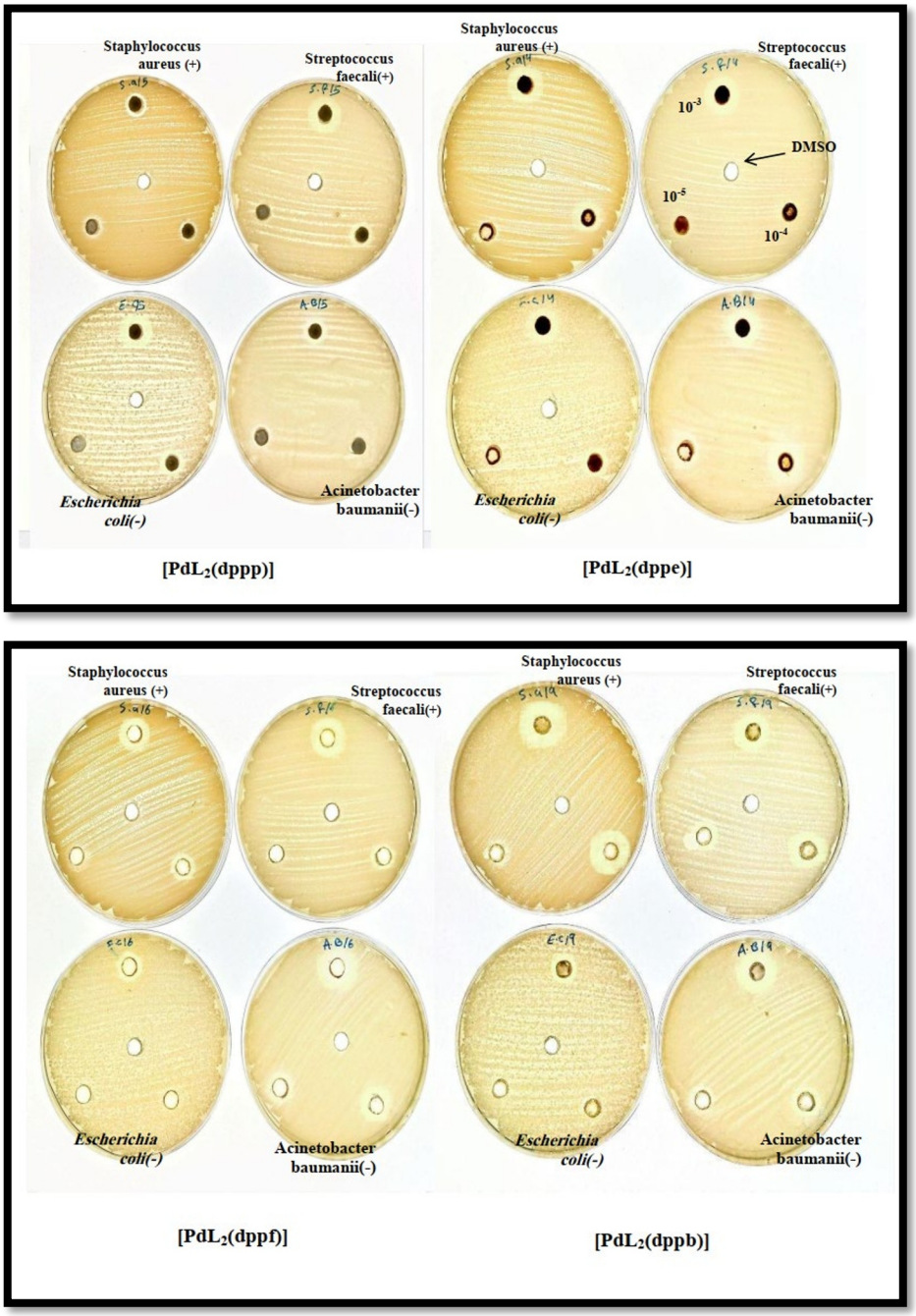

Fig. 6. The antibacterial inhibitory activity of the prepared complexes.

4 Conclusion

In this study, a new series of palladium (II) complexes incorporating 5-benzylthion-1H-tetrazole and various diphosphine ligands were successfully synthesized and

comprehensively characterized using spectroscopic techniques (FT-IR, NMR), conductivity measurements, and SEM/EDX analysis. The data confirmed the monodentate coordination mode of the tetrazole-thione ligand through the nitrogen atom, leading to square planar geometry around the Pd (II) center. SEM and EDX analyses revealed that the resulting complexes exhibit well-defined nanostructures with narrow size distributions, suggesting their potential applicability in nanotechnology-related fields, such as catalysis and materials science. Biological screening of the synthesized complexes demonstrated notable antibacterial activity against both Gram-positive and Gram-negative bacterial strains, with varying degrees of inhibition dependent on the ligand environment and concentration. Complexes such as [PdL_2(dppf)] and [PdL_2(dppb)] exhibited superior antibacterial efficacy, indicating that ligand architecture plays a significant role in biological performance. Overall, this study highlights the promising structural, nanoscale, and biological properties of tetrazole-thione-based palladium complexes, establishing a foundation for further exploration of their applications in antimicrobial therapy, catalysis, and advanced material design.

References

1. Popova, E. A., Trifonov, R. E., and Ostrovskii, V. A., Advances in the synthesis of tetrazoles coordinated to metal ions. Ark. Online J. Org. Chem. **2012**, (2012).
2. Alshargabi, A., Diclofenac derivatives as promising anticancer and anti-inflammatory drug: synthesis, formulations, and pharmacokinetics. J. Drug Deliv. Sci. Technol. **2024**, 105544 (2024).
3. Katritzky, A. R., Ramsden, C. A., Joule, J. A., and Zhdankin, V. V., Handbook of heterocyclic chemistry. Elsevier, (2010).
4. Raper, E. S., Complexes of heterocyclic thione donors. Coord. Chem. Rev. **61**, 115–184 (1985).
5. Raper, E. S., Copper complexes of heterocyclic thioamides and related ligands. Coord. Chem. Rev. **129**, 91–156 (1994).
6. Raper, E. S., Complexes of heterocyclic thionates. Part 1. Complexes of monodentate and chelating ligands. Coord. Chem. Rev. **153**, 199–255 (1996).
7. Raper, E. S., Complexes of heterocyclic thionates Part 2: complexes of bridging ligands. Coord. Chem. Rev. **165**, 475–567 (1997).
8. Akrivos, P. D., Recent studies in the coordination chemistry of heterocyclic thiones and thionates. Coord. Chem. Rev. **213**, 181–210 (2001).
9. Frija, L. M. T., Pombeiro, A. J. L., and Kopylovich, M. N., Coordination chemistry of thiazoles, isothiazoles and thiadiazoles. Coord. Chem. Rev. **308**, 32–55 (2016).
10. Lobana, T. S., Heterocyclic-2-thione derivatives of group 10–12 metals: Coordination versatility, activation of CS (thione) bonds and biochemical potential. Coord. Chem. Rev. **441**, 213884 (2021).
11. Shaker, R. M., The chemistry of mercapto-and thione-substituted 1, 2, 4-triazoles and their utility in heterocyclic synthesis. Arkivoc **9**, 59–112 (2006).
12. Al-Janabi, A. S. M., Alheety, M. A., Osama'a, A. Y., Shaaban, S., Kibar, B., and Cacan, E., Anti-cancer and anti-fungal evaluation of novel palladium (II) 1-phenyl-1H-tetrazol-5-thiol complexes. Inorg. Chem. Commun. **121**, 108193 (2020).
13. Al-Janabi, A. S. M., Al-Samrai, O. A. Y., and Yousef, T. A., New palladium (II) complexes with 1-phenyl-1H-tetrazole-5-thiol and diphosphine Synthesis,

characterization, biological, theoretical calculations and molecular docking studies. Appl. Organomet. Chem. **34**, e5967 (2020).

14. Alsaiari, R. A., Kamel, M. M., and Mohamed, M. M., Corrosion Inhibition of Expired Cefazolin Drug on Copper Metal in Dilute Hydrochloric Acid Solution: Practical and Theoretical Approaches. Molecules **29**, 1157 (2024).
15. Kabi, A. K., et al., An introduction on evolution of azole derivatives in medicinal chemistry. Nanostructured Biomaterials: Basic Structures and Applications, 79–99 (2022).